Diabetologia (2022) 65:1687–1700
https://doi.org/10.1007/s00125-022-05756-9

ARTICLE

Islet amyloid polypeptide aggregation exerts cytotoxic and proinflammatory effects on the islet vasculature in mice

Joseph J. Castillo[1,2] · Alfred C. Aplin[1] · Daryl J. Hackney[1] · Meghan F. Hogan[1,2] · Nathalie Esser[1,2] · Andrew T. Templin[1,2] · Rehana Akter[1,2] · Steven E. Kahn[1,2] · Daniel P. Raleigh[3,4] · Sakeneh Zraika[1,2] · Rebecca L. Hull[1,2]

Received: 28 January 2022 / Accepted: 28 April 2022 / Published online: 25 July 2022

Abstract

Aims/hypothesis The islet vasculature, including its constituent islet endothelial cells, is a key contributor to the microenvironment necessary for normal beta cell health and function. In type 2 diabetes, islet amyloid polypeptide (IAPP) aggregates, forming amyloid deposits that accumulate between beta cells and islet capillaries. This process is known to be toxic to beta cells but its impact on the islet vasculature has not previously been studied. Here, we report the first characterisation of the effects of IAPP aggregation on islet endothelial cells/capillaries using cell-based and animal models.

Methods Primary and immortalised islet endothelial cells were treated with amyloidogenic human IAPP (hIAPP) alone or in the presence of the amyloid blocker Congo Red or the Toll-like receptor (TLR) 2/4 antagonist OxPAPc. Cell viability was determined0 along with mRNA and protein levels of inflammatory markers. Islet capillary abundance, morphology and pericyte coverage were determined in pancreases from transgenic mice with beta cell expression of hIAPP using conventional and confocal microscopy.

Results Aggregated hIAPP decreased endothelial cell viability in immortalised and primary islet endothelial cells (by 78% and 60%, respectively) and significantly increased expression of inflammatory markers *Il6*, *Vcam1* and *Edn1* mRNA relative to vehicle treatment in both cell types ($p<0.05$; $n=4$). Both cytotoxicity and the proinflammatory response were ameliorated by Congo Red ($p<0.05$; $n=4$); whereas TLR2/4-inhibition blocked inflammatory gene expression ($p<0.05$; $n=6$) without improving viability. Islets from high-fat-diet-fed amyloid-laden hIAPP transgenic mice also exhibited significantly increased expression of most markers of endothelial inflammation ($p<0.05$; $n=5$) along with decreased capillary density compared with non-transgenic littermates fed the same diet ($p<0.01$). Moreover, a 16% increase in capillary diameter was observed in amyloid-adjacent capillaries ($p<0.01$), accompanied by a doubling in pericyte structures positive for neuron-glial antigen 2 ($p<0.001$).

Conclusions/interpretation Islet endothelial cells are susceptible to hIAPP-induced cytotoxicity and exhibit a TLR2/4-dependent proinflammatory response to aggregated hIAPP. Additionally, we observed amyloid-selective effects that decreased islet capillary density, accompanied by increased capillary diameter and increased pericyte number. Together, these data demonstrate that the islet vasculature is a target of the cytotoxic and proinflammatory effects of aggregated hIAPP that likely contribute to the detrimental effects of hIAPP aggregation on beta cell function and survival in type 2 diabetes.

Keywords Amyloid · Beta cell · Endothelial cell · Inflammation · Islet amyloid polypeptide · Islet vasculature · Islets · Type 2 diabetes

✉ Rebecca L. Hull
rhull@uw.edu

[1] Department of Veterans Affairs Puget Sound Health Care System, Seattle, WA, USA

[2] Division of Metabolism, Endocrinology, and Nutrition, Department of Medicine, University of Washington, Seattle, WA, USA

[3] Department of Chemistry, Stony Brook University, Stony Brook, NY, USA

[4] Research Department of Structural and Molecular Biology, University College London, London, UK

Abbreviations

CTF	Cell Titer Fluor
ECM	Extracellular matrix
EM	Electron microscopy
HF	High-fat diet
hIAPP	Human IAPP
IAPP	Islet amyloid polypeptide
LF	Low-fat diet
LPS	Lipopolysaccharide

Research in context

What is already known about this subject?

- Islet amyloid polypeptide (IAPP) aggregation in type 2 diabetes is cytotoxic to beta cells
- IAPP aggregates accumulate as amyloid deposits in the extracellular matrix between beta cells and endothelial cells
- Islet vasculature is an important mediator of normal beta cell function/survival

What is the key question?

- Does IAPP aggregation negatively impact islet capillaries, specifically with respect to cell viability, morphology and inflammatory state?

What are the new findings?

- IAPP aggregation is cytotoxic to islet endothelial cells in vitro and results in islet capillary loss in vivo
- IAPP aggregation induces a Toll-like receptor-2/4-dependent proinflammatory response in cultured islet endothelial cells
- Islet capillaries adjacent to aggregated IAPP (amyloid deposits) exhibit an increased diameter and an increased number of neuron-glial antigen 2-positive pericyte structures per capillary

How might this impact on clinical practice in the foreseeable future?

- Development of therapies that can target islet vascular inflammation and dysfunction will likely improve beta cell function and survival in type 2 diabetes

MS-1	Immortalised mouse islet endothelial cell
NBF	Neutral buffered formalin
NG2	Neuron-glial antigen 2
NT	Non-transgenic
rIAPP	Rodent IAPP
ROIs	Regions of interest
TG	Transgenic
TLR	Toll-like receptor
VCAM-1	Vascular cell adhesion molecule-1
XTT	2,3-bis-(2-methoxy-4-nitro-5-sulfophenyl)-2H-tetrazolium-5-carboxanilide

Introduction

The pancreatic islet is supplied by a capillary network composed of fenestrated endothelial cells surrounded by contractile pericytes. The islet vasculature facilitates delivery of nutrients to beta cells and allows efficient distribution of islet hormones to the peripheral circulation. The islet endothelial cell has emerged as a key source of growth factors and extracellular matrix (ECM) molecules that support beta cell function, survival and proliferation [1–4]. Crosstalk between beta cells and islet endothelial cells is required for proper islet vascularisation and normal beta cell function [5–7]. In type 2 diabetes, islet capillaries are morphologically altered [8, 9]. Moreover, islet endothelial cells from cell or animal models of type 2 diabetes show an activated (inflammatory and pro-adhesive) phenotype [7, 10, 11], and are no longer able to adequately support beta cell function [7].

Following beta cell exocytosis, insulin and other beta cell products must cross the ECM and the endothelial cell itself to reach the circulation. Islet amyloid polypeptide (IAPP; amylin) is one such beta cell product, which aggregates in human type 2 diabetes to form islet amyloid deposits [12, 13].

The human form of IAPP (hIAPP) is amyloidogenic, while rodent IAPP (rIAPP) is not [14]. Therefore, to study IAPP aggregation in mice (or rats) it is necessary to utilise hIAPP transgenic (TG) animals. The cytotoxic effects of hIAPP aggregation on beta cells in the context of type 2 diabetes are well-documented [15–19]. hIAPP aggregation has also been shown to elicit an inflammatory response from macrophages [20–22]. However, while it has long been appreciated that hIAPP deposition occurs between beta cells and islet capillaries [23–25], whether aggregated hIAPP can also exert toxic/proinflammatory effects on the islet vasculature remains unknown. Support for such an effect comes from studies in pancreases from humans with type 2 diabetes, where disturbed capillary morphology was preferentially seen in areas close to islet amyloid deposits [8] and islet capillary density was selectively decreased in islet amyloid-positive individuals with type 2 diabetes [26]. An electron microscopy (EM) study in hIAPP ('HIP') TG rats also reported morphological

abnormalities in the vasculature of amyloid-laden islets [27]. Here, we used cell and animal-based models to test the hypothesis that aggregation of amyloidogenic hIAPP results in islet vasculopathy and inflammation.

Methods

Isolation and culture of islet endothelial cells Immortalised mouse islet endothelial cells (MS-1; accession number CVCL_6502) were maintained in RPMI 1640 medium containing 11.1 mmol/l glucose, 10% FBS, 1 mmol/l sodium pyruvate, 100 U/ml penicillin and 100 μg/ml streptomycin ('complete media'; all components from Invitrogen, ThermoFisher Scientific, USA).

Primary rat islet endothelial cells were obtained from Sprague Dawley rat islets, which were dissociated to single cells and subjected to anti-CD31 antibody magnetic bead sorting (Miltenyi Biotec, USA; see electronic supplementary material [ESM] Methods and ESM Fig. 1).

MS-1 and primary islet endothelial cells were distributed into individual wells of either 24- or 96-well dishes at 15,000 cells/cm^2. Cells were cultured in complete RPMI media for 7 days prior to addition of test reagents. Cell lines were negative for presence of mycoplasma by PCR-based detection of 16S RNA using the MycoStrip Mycoplasma Detection Kit (InvivoGen, USA)

Preparation of IAPP and treatment of cultured cells Human and rodent IAPP peptides were synthesised [28] or purchased (Creative Biomart, USA or Bachem, USA), reconstituted in 1-1-1-3 hexafluoroisopropanol (Sigma-Aldrich, USA) to ensure the absence of aggregates and lyophilised in 100 μg aliquots. IAPP was then resuspended in Tris-HCl buffer (20 mmol/l, pH 7.4) and diluted into complete media at final concentrations from 1 to 20 μmol/l immediately prior to use.

To block aggregation of IAPP, the azo dye Congo Red (Sigma-Aldrich) was prepared in DMSO (0.1% vol./vol.). Congo Red (200 μmol/l) or vehicle was added to complete media prior to IAPP addition. The expected effect of Congo Red, to prevent hIAPP aggregation under these conditions, was confirmed by thioflavin T assay and transmission EM (ESM Methods and ESM Fig. 2).

The Toll-like receptor (TLR)-4 agonist lipopolysaccharide (LPS, Sigma-Aldrich) or TLR2 agonist Pam3CSK4 (InvivoGen) was added to complete media at 10 μg/ml. For TLR blocking studies, the TLR2/4 antagonist OxPAPc (30 μg/ml; InvivoGen) was added to complete media prior to IAPP addition.

Cell viability assays Cell viability was determined using a cell proliferation assay (2,3-bis-[2-methoxy-4-nitro-5-sulfophenyl]-2H-tetrazolium-5-carboxanilide or XTT; ThermoFisher) or Cell Titer Fluor (CTF; Promega, USA) assays. The CTF assay was used in experiments containing Congo Red, as the latter interferes with the colorimetric detection of formazan produced by the XTT reaction. In the absence of Congo Red, XTT and CTF assays generated interchangeable data (not shown).

Gene expression analysis RNA was harvested from cells (High Pure RNA Kit; Roche, USA) and reverse transcribed (High-Capacity cDNA Reverse Transcription Kit; ThermoFisher). Islet cDNA from amyloid-containing hIAPP (TG) and non-transgenic (NT) littermate control mice after 1 year on high- or low-fat diet were available from a previous study [22]. cDNAs were analysed, in triplicate, using pre-validated TaqMan primer-probes (Applied Biosystems, USA, ESM Table 1). Results were calculated with *Ppib* as the housekeeping gene using the $2^{-\Delta\Delta C_t}$ method.

Protein analyses Cell culture media were collected for measurement of IL-6 (V-PLEX Mouse IL-6 Kit; Meso Scale Diagnostics, USA) and endothelin-1 (no. EM26RB, ThermoFisher). Protein values were normalised to the number of cells determined from CTF assay data.

For western blotting, cell lysates (20 μg/sample) were separated on 4–20% polyacrylamide gels (BioRad, USA) and transferred to nitrocellulose (BioRad). Blots were probed with antibody to vascular cell adhesion molecule-1 (VCAM-1; 1:2000; ab134047, Abcam, USA) and β-actin (goat anti-rabbit 1:3000; ab227387, Abcam), followed by horseradish-peroxidase-conjugated secondary antibody (goat anti-rabbit, 1:3000; ab6721, Abcam) and SuperSignal West Femto Maximum Sensitivity Substrate kit (ThermoFisher). Antibodies were validated based on presence of immunoreactive band at the expected molecular weight, lack of band in negative controls (omission of primary antibody) and presence in positive controls (multiple historical samples for β-actin and inflamed endothelial cells for VCAM-1).

Mouse model, vascular labelling and pancreas harvest All studies were approved by the VA Puget Sound Institutional Animal Care and Use Committee, performed in an AAALAC-accredited animal research facility, and adhered to the Animal Research: Reporting of In Vivo Experiments (ARRIVE) guidelines.

Male hemizygous hIAPP TG mice (generated as described in [29]), along with NT littermates on a B6D2 background (B6D2-Tg(RIP-hIAPP)CStka) were consecutively assigned to study until there were eight mice per genotype; no animals were removed from study. Mice were fed a diet with 18% energy from fat (9% wt/wt) (PicoLab Mouse Diet 20 5058; Purina Lab Diet, USA) for an average of 14.7 months (ESM Table 2), which is sufficient to induce pancreatic islet amyloid deposition along with impaired insulin release and beta cell

mass [30]. TG mice do not develop overt diabetes at this age [22, 30] (hyperglycaemia is more frequent at ~18 months [25]). This is advantageous in the present study as it permits investigation of the impact of amyloid formation without the confounding effect of hyperglycaemia.

For generation of frozen pancreas blocks for histology, mice were anaesthetised with sodium pentobarbital (100 mg/kg i.p.). Lectin (Dylight 649-conjugated *Lycopersicon esculentum*, 2 mg/ml; Vector Laboratories, USA) was infused into the inferior vena cava and allowed to circulate for 5 min prior to perfusion fixation with 10% neutral buffered formalin (NBF, VWR International, USA). Pancreases were excised, postfixed overnight in 10% NBF, infiltrated with sucrose (30%) and frozen in optimal cutting temperature (OCT) media (Tissue Tek, Sakura, USA). Sections, 4 and 30 μm thick, were cut for wide-field fluorescence and confocal microscopy, respectively.

Immunohistochemistry Antibodies for CD31, insulin, neuron-glial antigen 2 (NG2) and VCAM-1 immunohistochemistry were selected based on extensive validation in-house and/or in the literature. The expected localisation of immunoreactivity for these antigens is well established (endothelial cells for CD31, beta cells for insulin and perivascular pericytes for NG2). VCAM-1 is known to be selectively localised to inflamed endothelium. We performed IgG isotope negative controls for all antibodies.

Paraffin-embedded pancreas sections, 4 μm thick, were utilised from our previously published study [22]. Automated immunostaining (BOND-Max; Leica Biosystems, IL, USA) was performed with heat-mediated EDTA antigen retrieval (100°C for 20 min), followed by anti-CD31 antibody (1:250; DIA-310; Dianova, Germany) and rabbit anti-rat IgG (1:3000; AI-4001; Vector Laboratories). Immunoreactivity was visualised using Leica Bond Mixed Refine reagents (Leica Biosystems) with haematoxylin counterstaining. For VCAM-1 staining, sections were treated with heat-mediated EDTA antigen retrieval (10 min), followed by anti VCAM-1 antibody (1:500; ab134047; Abcam) and Leica Bond Mixed Refine polymer/chromagen. Sections were counterstained with thioflavin S (1% wt/vol.; Sigma-Aldrich) to visualise amyloid deposits.

For confocal microscopy, 30 μm frozen sections were immunostained for insulin (1:50; A0564; Dako/Agilent, CA, USA) with AlexaFluor-546 conjugated goat anti-rabbit IgG (1:200; A-11004; Invitrogen), followed by thioflavin S counterstaining.

Pericyte staining was done on 4 μm frozen sections incubated with antibody to NG2 (1:100; AB5320; EMD Millipore, USA) followed by Alexa-fluor 568 conjugated goat anti-rabbit IgG (1:200; A11011; Invitrogen) and thioflavin S counterstaining.

For immunostaining visualised by confocal microscopy, sections were blocked for 1 h in buffer containing 0.05 mol/l PBS (Gibco, ThermoFisher Scientific), 0.2% wt/vol. Triton X-100 (Sigma-Aldrich), 0.01% wt/vol. sodium azide (Sigma-Aldrich), 1% wt/vol. BSA (Sigma-Aldrich) and 2% normal goat serum (Vector Laboratories, USA). Antibodies were diluted in buffer containing 0.05 mol/l PBS, 0.2% wt/vol. Triton X-100, 0.01% sodium azide and 1% wt/vol. BSA.

Microscopy and image analysis For CD31 immunohistochemistry, brightfield images were generated (NiE microscope; Nikon Instruments, USA) using ×10 objective magnification, and stitched to generate a whole-slide image (Nikon NIS Elements HC). Islets (15±2 per mouse, mean±SEM) were hand-circled to generate regions of interest (ROIs). Binary thresholding was used to generate CD31-positive areas and object counts. Experimenters were blind to group assignment.

Analysis of capillary density and morphology was done by confocal microscopy (A1R-HD; Nikon). Imaging parameters are provided in ESM Methods. Briefly, islet z-stacks were compiled for analysis of capillaries (lectin) and amyloid deposits (thioflavin S). Capillary images (~100 per islet) were obtained for five islets, selected at random from different regions of the pancreas, per mouse, yielding samples sizes comparable with those of recent studies [31–34]. Morphometric analyses were done using Volocity software (Quorum Technologies, Lewes, UK), as described in ESM Methods. Capillary and amyloid volume and capillary density measurements were calculated on a per-mouse basis and for amyloid-adjacent vs non-adjacent capillaries (defined in ESM Methods). Experimenters were blind to group assignment.

Pericyte (NG2) staining was imaged via wide-field fluorescence microscopy (Ti2; Nikon; image acquisition and analysis parameters are described in ESM Methods). NG2-, lectin- and thioflavin S-positive pixels within islet ROIs (57±5 islets/mouse) and in amyloid-adjacent and non-adjacent capillaries were analysed to generate NG2- and lectin-positive areas and object counts. Object counts, morphometric analysis, and density measurement data were collected by observers blinded to the identity of experimental groups.

Statistical analyses Data are presented as mean ± SEM. One-way ANOVA with Dunnett's multiple comparisons test was used to detect significant differences in outcome measures for cells cultured with or without hIAPP/rIAPP, and morphometric analyses. Two-way ANOVA with Sidak's multiple comparisons test was used to determine differences between conditions with or without Congo Red and OxPAPc, and mRNA data from mouse islets. Student's *t* test was used for two-group comparisons. Prism (version 9.3; GraphPad Software, USA) was used for all statistical analyses.

Numbers of experimental replications are represented by individual data points in figures.

Results

hIAPP treatment decreases cell viability and upregulates inflammatory proteins in immortalised and primary islet endothelial cells To determine a working concentration of hIAPP for further study, we generated a dose–response curve using immortalised islet endothelial cells (MS-1 cell line). MS-1 cells treated with hIAPP exhibited decreased cell viability, with 50% and 78% decreases in viability seen with 10 μmol/l and 20 μmol/l hIAPP, respectively (Fig. 1a) and upregulation of mRNA for the inflammatory marker *Il6*, the cell adhesion molecule *Vcam1* and the vasoconstrictor *Edn1* (Fig. 1b–d), all of which have previously been shown to be increased in islet endothelial cells in animal models of type 2 diabetes [7, 10, 11]. Based on these data, we selected a concentration of 20 μmol/l hIAPP for the remaining studies. MS-1 cells treated with hIAPP were next compared with non-amyloidogenic rIAPP as a negative control. hIAPP-treated but not rIAPP-treated islet endothelial cells displayed decreased cell viability (Fig. 1e), increased IL-6 secretion (Fig. 1f) and increased VCAM-1 protein expression (Fig. 1g).

Treatment of primary islet endothelial cells with hIAPP also resulted in a 60% decrease in cell viability (Fig. 2a) and increases in *Il6*, *Vcam1*, and *Edn1* mRNA (Fig. 2b–d) compared with treatment with rIAPP or vehicle control.

Blocking hIAPP aggregation ameliorates its cytotoxic and proinflammatory effects in immortalised islet endothelial cells To delineate between effects of the hIAPP monomer and its aggregated forms, we blocked hIAPP aggregation by co-treatment with Congo Red, which is known to inhibit the formation of β-sheet fibrils by amyloidogenic peptides, including hIAPP [35, 36] (ESM Fig. 2). Congo Red prevented the hIAPP-mediated decrease in cell viability (Fig. 3a), blocked the increase in *Vcam1*, *Il6* and *Edn1* mRNA (Fig. 3b–d), and prevented the increase in secreted IL-6 (Fig. 3e) and endothelin-1 (Fig. 3f).

Proinflammatory response of islet endothelial cells to hIAPP is dependent on TLR2 and TLR4 Since the innate immune receptor TLR2 has been identified as a mediator of hIAPP response in macrophages [37] and TLR4 activation contributes to inflammation and upregulation of IL-6 in macrophages [38], we next determined the role of TLR2/4 in the islet endothelial cell response to hIAPP treatment. First, we verified that MS-1 cells express *Tlr2* and *Tlr4*

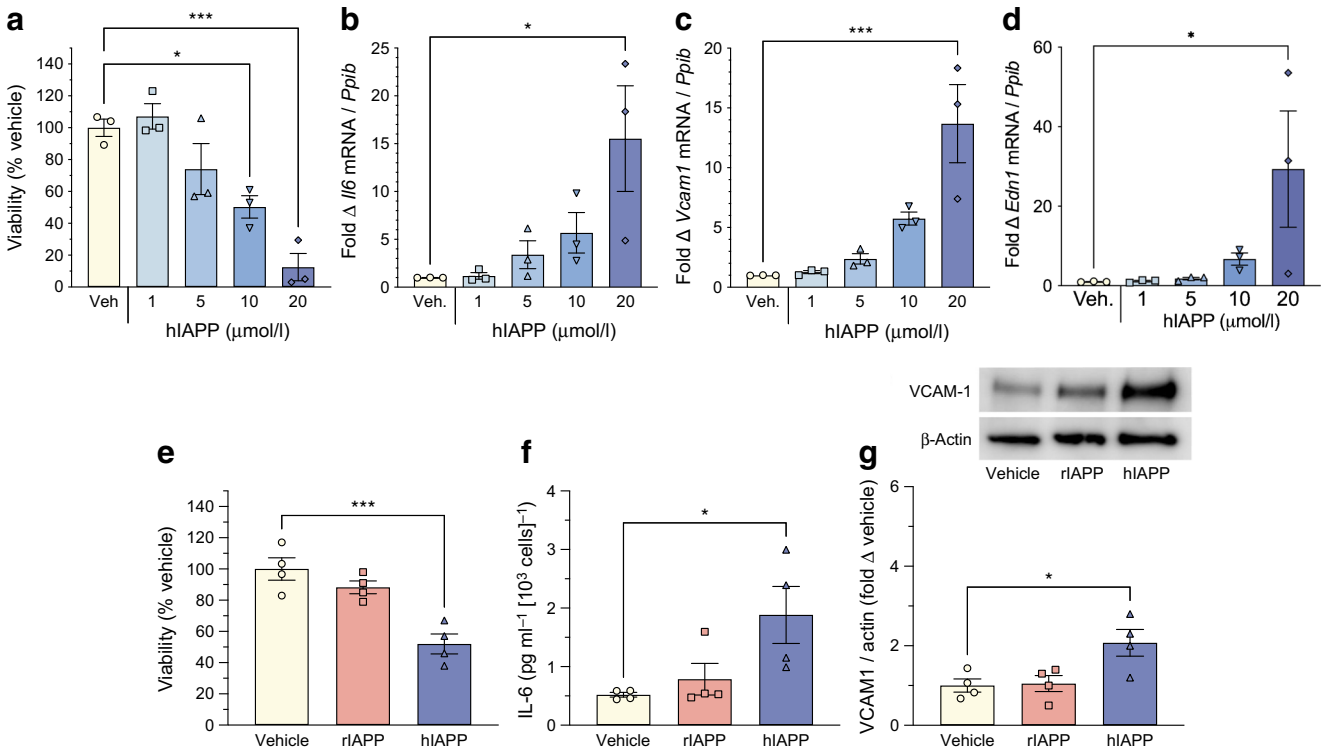

Fig. 1 Dose–response curve for hIAPP treatment of MS-1 cells. (**a**–**d**) Cell viability (**a**) and relative gene expression of endothelial dysfunction markers *Il6* (**b**), *Vcam1* (**c**) and *Edn1* (**d**) after treatment for 48 h with vehicle (Veh.; Tris buffer) or hIAPP (1–20 μmol/l). n=3; *p<0.05 and ***p<0.001. (**e**–**g**) Cell viability (**e**) and levels of IL-6 protein in media (**f**) or VCAM-1 protein in cell lysate (**g**) from MS-1 cells treated for 48 h with vehicle (Tris buffer), rIAPP (20 μmol/l) or hIAPP (20 μmol/l). n=4; *p<0.05 and ***p<0.001

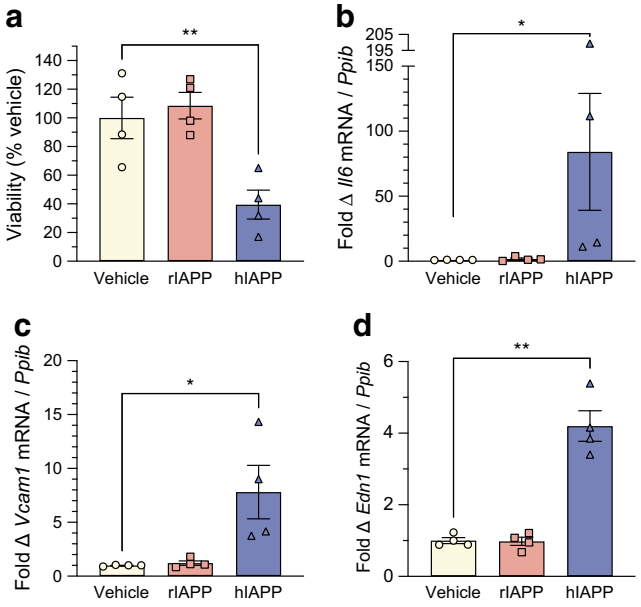

Fig. 2 Cell viability (**a**) and relative gene expression of *Il6* (**b**), *Vcam1* (**c**) and *Edn1* (**d**) in primary islet endothelial cells treated for 48 h with vehicle (Tris buffer), rIAPP (20 μmol/l) or hIAPP (20 μmol/l). n=4; *p<0.05 and **p<0.01

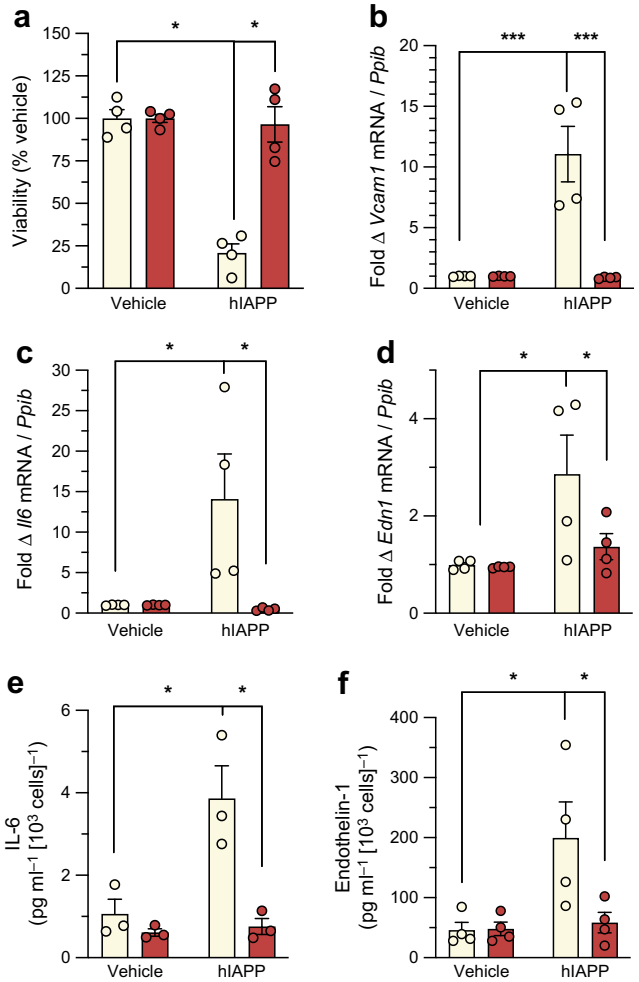

Fig. 3 Cell viability (**a**) and relative gene expression of *Vcam1* (**b**), *Il6* (**c**) and *Edn1* (**d**), as well as levels of IL-6 protein (**e**) and endothelin-1 protein (**f**) secreted from MS-1 cells exposed for 48 h to vehicle or hIAPP (20 μmol/l), in DMSO vehicle (white bars) or with Congo Red (red bars). n=4; *p<0.05 and ***p<0.001

(ESM Fig. 3a, b). In response to hIAPP treatment, *Tlr2* expression was significantly decreased, while *Tlr4* expression was induced. Second, we confirmed that stimulation of TLR2 and TLR4 in MS-1 cells (using Pam3CKS4 and LPS, respectively) was capable of inducing an inflammatory response as demonstrated by an increase in expression of *Il6* and *Vcam1*, but not *Edn1*, without substantial cytotoxicity (ESM Fig. 3d–f).

MS-1 cells were then treated with hIAPP in the presence or absence of the TLR2/4 antagonist OxPAPc. This antagonist did not rescue cell viability (Fig. 4a) but was effective in blocking upregulation of *Il6*, *Vcam1* and *Edn1* compared with hIAPP alone (Fig. 4b–d).

Markers of endothelial inflammation and dysfunction are upregulated in amyloid-laden islets ex vivo To determine whether there was evidence of endothelial inflammation in amyloid-laden islets from an in vivo mouse model, we used islet cDNAs from a previously published cohort of amyloid-positive high-fat diet (HF)-fed TG mice along with low-fat diet (LF)-fed TG and NT littermate control mice [22]. *Il6* mRNA levels from HF-fed TG mouse islets were significantly increased when compared with islets from LF-fed TG mice (Fig. 5a; p<0.001) and HF-fed NT mice (p<0.001). In contrast, no difference was detected in islets from HF-fed NT vs LF-fed NT mice. A similar expression pattern was observed for *Sele* (encoding for E-selectin, a vascular cell adhesion molecule) mRNA (Fig. 5b), while *Edn1* mRNA (Fig. 5c) was not significantly increased in HF-fed TG mouse islets.

Amyloid-laden islets display reduced capillary density Pancreas sections from the same mice used to isolate islet cDNA were then analysed by CD31 immunohistochemistry. Representative images show VCAM-1 immunohistochemistry in islets from HF-fed NT and HF-fed TG mice (Fig. 5d,e), with a substantial increase in VCAM-1 immunoreactivity being observed in capillaries close to amyloid deposits (Fig. 5e, arrowheads). CD31 immunohistochemistry shows representative examples of islet capillary morphology in islets from HF-fed NT and HF-fed TG mice (Fig. 5f,g). As expected, mean islet area was increased in both NT and TG mice on HF, compared with LF-fed mice for each genotype (Fig. 5h). There was no difference among the groups in CD31-positive area expressed as a percentage of islet area (Fig. 5i). Islet capillary density was similar for LF-fed mice (NT and TG), while HF-fed NT mice displayed significantly higher capillary density compared with LF-fed NT mice. In contrast, HF-fed TG mice showed no increase in capillary density relative to

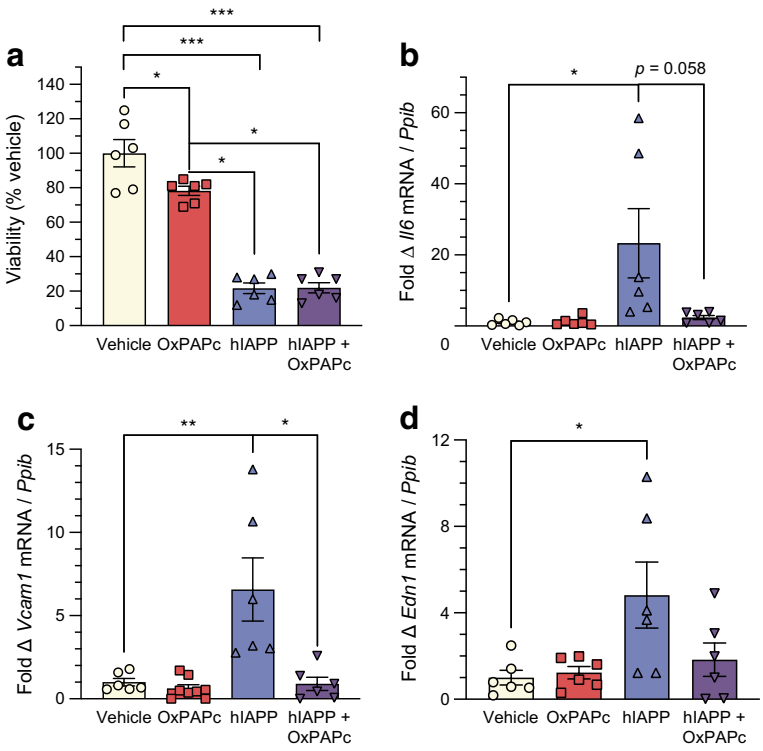

Fig. 4 Cell viability (**a**) and relative gene expression of *Il6* (**b**), *Vcam1* (**c**) and *Edn1* (**d**) from MS-1 cells treated with vehicle (RPMI media) or with OxPAPc, hIAPP, or both, for 48 h. n=6; *p<0.05, **p<0.01 and ***p<0.001

LF-fed TG mice and islet capillary density was significantly decreased in HF-fed TG vs HF-fed NT mice (Fig. 5j), despite similar islet area.

Islet amyloid deposits are closely associated with islet capillaries To determine in greater detail the impact of amyloid deposition on islet vasculature, we labelled blood vessels in situ with fluorescent lectin in both TG and NT mice fed HF for 1 year. Representative confocal images of pancreas sections from both genotypes (Fig. 6a,b) clearly demonstrated the close association of amyloid deposits to islet capillaries in TG mouse islets (Fig. 6b,c and ESM Video).

Amyloid-laden islets exhibit reduced capillary density and increased capillary diameter Islet amyloid was detected in all TG mice (Fig. 7a). In line with the data from CD31 immunohistochemistry, no difference was seen in mean islet volume between TG and NT mouse islets (Fig. 7b) and quantification of capillary volume as a percentage of islet volume was also similar between genotypes (Fig. 7c). Capillary density, however, was significantly diminished in TG mice (Fig. 7d). When all capillaries were compared between genotypes, neither mean volume nor mean diameter differed (Fig. 7e,f). However, when capillaries within TG mouse islets were categorised based on their proximity to amyloid deposits (using ≤10 μm distance as the cut-off to define amyloid-adjacent capillaries), mean volume was not significantly different (Fig. 7g), while mean diameter was significantly larger (Fig. 7h) in amyloid-adjacent capillaries. Further, a 16% increase in capillary diameter was only observed in capillary structures that were ≤10 μm from amyloid, compared with capillaries that were more distant from amyloid deposits (ESM Fig. 4).

The pericyte/capillary ratio is increased in amyloid-laden islets Pericytes are the constrictive cell type within islet capillaries. Given our observation of increased capillary diameter with amyloid deposition, and increased expression/secretion of *Edn1*/endothelin-1 from hIAPP-treated islet endothelial cells (Figs 1d, 2d, 3d,f, 4d and 5c), we hypothesised that islet amyloid deposition might be associated with loss of islet pericytes. Representative images from mouse pancreas sections stained with lectin (capillary), anti-NG2 (pericyte) and thioflavin S (amyloid) are shown in Fig. 8a,b. The mean area of islet capillaries did not differ by genotype (Fig. 8c). However, the number of NG2-positive structures (NG2 objects) per capillary (lectin objects) was increased in TG relative to NT mouse islets (Fig. 8d), while the pericyte area normalised to capillary area did not differ between genotypes (Fig. 8e). Consistent with the data presented above, in TG mice we found that the capillaries that were adjacent to amyloid deposits were significantly larger (Fig. 8g). Finally, within TG mice, the number of NG2-positive structures per capillary was doubled (Fig. 8h) while the NG2-positive area did not differ (Fig. 8i) when comparing amyloid-adjacent islet capillaries with non-amyloid-adjacent capillaries.

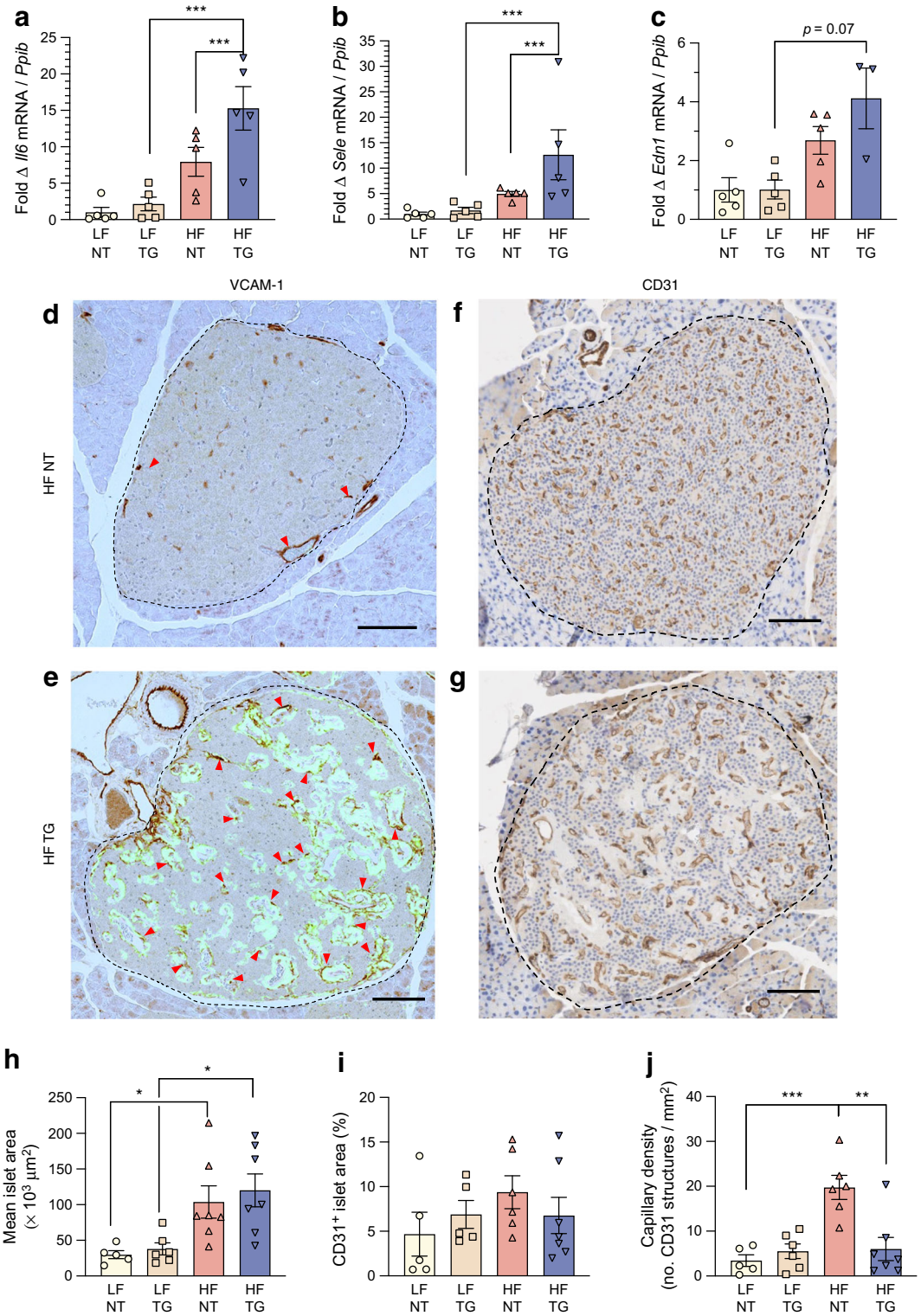

Fig. 5 (**a**–**c**) Relative gene expression of *Il6* (**a**), *Sele* (**b**) and *Edn1* (**c**) from whole islets isolated from NT and TG mice after 1 year on LF or HF. Values are shown as fold change relative to the LF-fed NT group. (**d**–**j**) Representative images of HF-fed NT (**d**, **f**) and HF-fed TG (**e**, **g**) mouse pancreas sections stained with anti-VCAM-1 (**d**, **e**; brown) or anti-CD31 (**f**, **g**; brown) together with counterstaining with haematoxylin (**d**, **e**, **f**, **g**; blue) and/or thioflavin S (**d**, **e**; green). The dashed lines denote islet boundary; red arrows denote positive VCAM-1 staining. Scale bars, 100 µm. Mean islet area (**h**), percentage of CD31-positive area per islet area (**i**) and capillary density (**j**) of the pancreas sections were determined. n=5–7 mice/group; *p<0.05, **p<0.01 and ***p<0.001

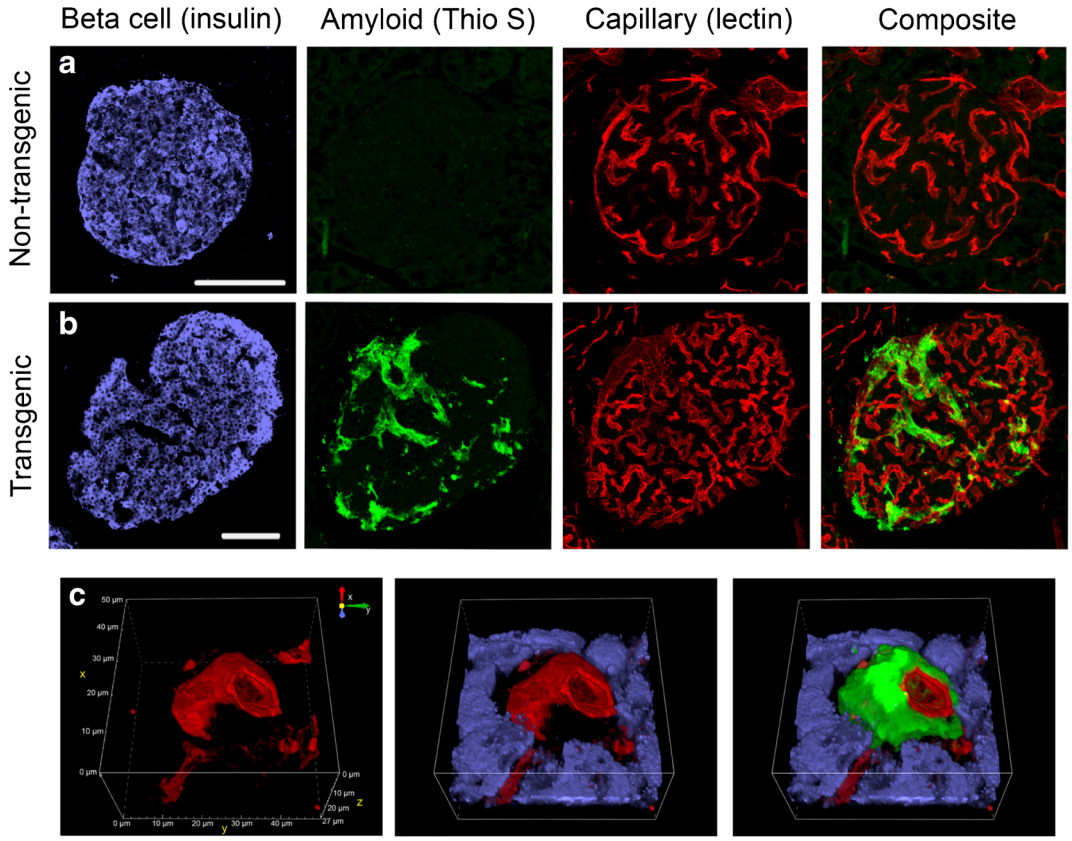

Fig. 6 (**a**, **b**) Representative confocal images from 30 μm-thick pancreas sections from NT (**a**) and TG mice (**b**) after 1 year of high-fat feeding showing islets visualised with insulin immunohistochemistry (purple). Amyloid deposits (thioflavin [Thio] S; green) and capillaries (lectin; red) are shown individually and as a composite image. Scale bar, 100 μm. (**c**) Higher magnification volume view of a TG mouse islet capillary (red) illustrating relative proximity to amyloid (green) and beta cells (purple)

Discussion

The cytotoxic effects of islet amyloid deposition on beta cells are well known [15–19]. However, the effect of hIAPP aggregation/islet amyloid on the islet vasculature has not previously been explored, aside from a single EM study in hIAPP TG rats [27]. Here, we present the first detailed investigation into the impact of hIAPP aggregation on cultured endothelial cells and on islet capillaries in vivo. In doing so, we have identified islet endothelial cells as a novel target of hIAPP cytotoxicity and show that hIAPP aggregation is required to induce cytotoxicity in vitro. We also demonstrate that amyloid induces a proinflammatory phenotype that is mediated by TLR2/4. In vivo, we show that amyloid aggregation is associated with increased VCAM-1 immunoreactivity and decreased capillary density, along with increased capillary diameter and an increase in NG2-positive pericyte structures along microvessels adjacent to amyloid deposition. These amyloid-induced disruptions of the islet vasculature may contribute to the progression of diabetes through effects on blood flow within the islet, impairment of insulin release and/or increase in the inflammatory burden within the islet.

The amyloid inhibitor Congo Red was effective in blocking both the cytotoxic and proinflammatory effects of hIAPP on endothelial cells, suggesting that aggregation/fibrillogenesis is the key contributing factor. This is consistent with data from studies of the effects of Aβ peptide aggregation on brain microvascular endothelial cells, showing the peptide to be toxic only in its aggregated form [39]. Additionally, our in vitro data demonstrate that the toxic effect of aggregated IAPP on endothelial cells does not occur secondary to well-known amyloidogenic effects on beta cells, suggesting that the cytotoxic effect on endothelial cells is direct.

We sought to determine whether the proinflammatory effect of hIAPP on endothelial cells is dependent on similar mechanisms known to govern inflammatory responses in islet macrophages, including in response to hIAPP, namely TLR2 and TLR4 [37, 38]. In the present study, we confirmed that both TLR2 and TLR4 are present on cultured islet endothelial cells and that TLR2 and 4 agonists can induce a proinflammatory response in those cells. Furthermore, a TLR2/4 antagonist effectively blocked the islet endothelial cell's proinflammatory response to hIAPP but was ineffective in blocking

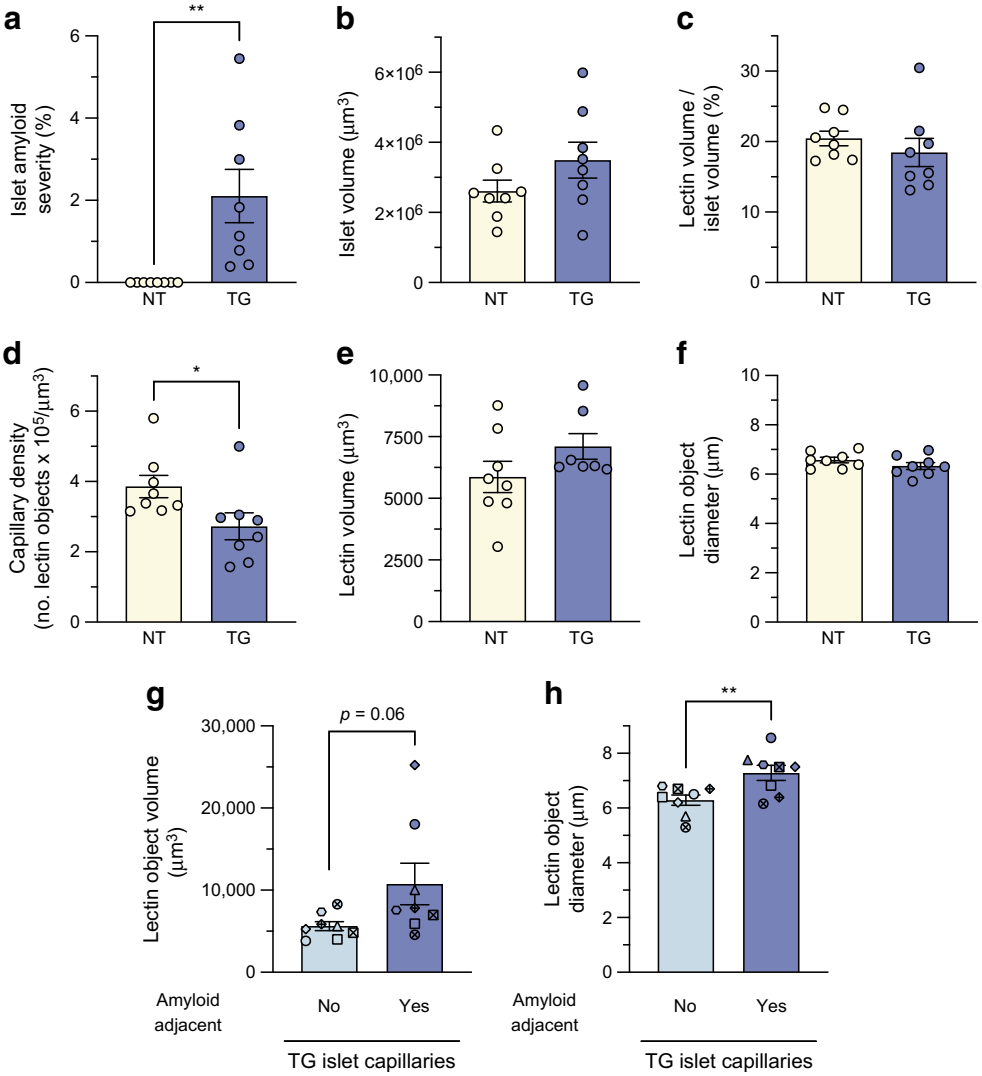

Fig. 7 (**a**–**f**) Mean amyloid severity (% volume per islet; **a**), mean islet volume (**b**), mean lectin islet volume % (**c**), capillary density (**d**), mean volume of lectin-positive capillary structures (**e**) and mean diameter of lectin-positive capillary structures (**f**) in pancreas sections from NT or TG mice after 1 year on HFD. (**g**, **h**) Mean volume (**g**) and mean diameter (**h**) of non-amyloid-adjacent and amyloid-adjacent islet capillary structures in TG mice (same symbol in each bar represents data point from same mouse). n=8 mice/group, 5 islets/mouse; *p<0.05 and **p<0.01

hIAPP cytotoxicity. This indicates that mechanisms underlying the proinflammatory and cytotoxic effects of hIAPP on islet endothelial cells are distinct and/or that the proinflammatory effects of hIAPP are downstream of cytotoxicity. A plausible mechanism for the latter would be that aggregated hIAPP first acts to destabilise cell membranes, an established mechanism for amyloid-induced cytotoxicity [18, 40–42]. This could result in generation and release of damage-associated molecular patterns (DAMPs), which in turn could elicit a TLR 2/4-mediated proinflammatory response [43].

Deposition of islet amyloid in vivo in hIAPP TG mice is also associated with increased expression of the same proinflammatory markers identified in the aforementioned in vitro studies, along with E-selectin, a response which also mirrors that seen in islet endothelial cells in *db/db* diabetic mice [7, 11]. This proinflammatory effect of islet amyloid on endothelial cells likely contributes to the overall inflammatory milieu within islets in the diabetic state. However, it should be noted that the present mRNA analysis was performed on whole islets, and specific-cell-type expression of inflammatory genes was not determined.

We also examined the morphological effects of amyloid deposition on the islet vasculature in vivo. Islets from obese mice, including HF-fed hIAPP TG and NT mice, become enlarged over time [31, 44]. Intra-islet vasculature has been reported to expand under these same conditions in mice [31, 45], as observed in the HF-fed NT mice studied here. Increased islet vascular density has also been reported in pancreas from humans with type 2 diabetes [8, 9, 46]. However, when amyloid is taken into account, a selective decrease in islet capillary density is observed [26]. In line with this latter finding, amyloid deposition was also associated with decreased islet vascular density in hIAPP TG mice in the present study. This suggests that amyloid deposition has a negative effect on vascular density in vivo, perhaps caused by vessel fragmentation, rarefaction or cell death. Alternatively, amyloid deposition may inhibit angiogenesis

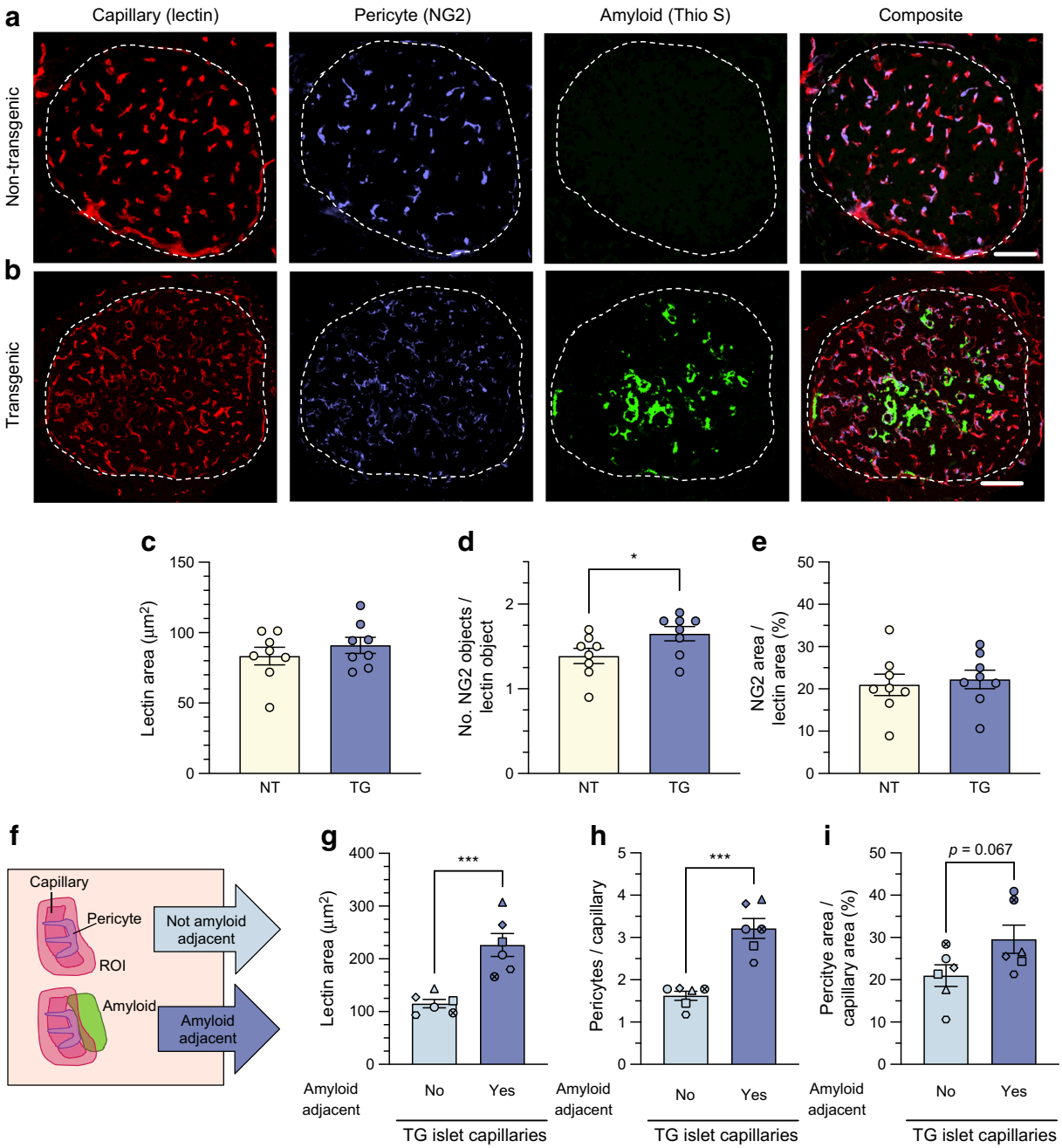

Fig. 8 (**a**, **b**) Representative images of islets from NT (**a**) and TG (**b**) mice in 4 µm-thick pancreas sections stained with lectin (capillaries, red), anti-NG2 (pericytes, purple), thioflavin [Thio] S (amyloid, green) and composite. Scale bar, 100 µm. (**c**–**e**) Lectin object area (i.e. individual capillary area; **c**), NG2 object (pericytes)/lectin object (capillaries) ratio (no. of pericyte structures per capillary; **d**) and percentage NG2 area/lectin area (**e**) were quantified from these and similar images. (**f**) Diagram showing dichotomous categorisation of TG capillaries based on proximity to amyloid. (**g**–**i**) Mean lectin object area (single capillary area; **g**), NG2 object count/lectin object count ratio (no. of pericyte structures per capillary; **h**) and percentage of NG2 area/lectin area (**i**) were computed for all TG mouse capillaries (same symbol in each bar represents same mouse). n=6 mice; *p<0.05 and ***p<0.001

within the islet as the beta cell population expands, consistent with reports of anti-angiogenic effects of amyloid-β in the brain [39, 47].

Amyloid deposition in our model is heterogenous, both within and between individual islets. This is consistent with the pattern of amyloid deposition seen in diabetic human pancreas [8, 19] and in previous studies using this hIAPP TG mouse model [48, 49]. When the overall morphology of islet capillaries was examined, we did not observe any difference in vessel size/diameter between islets from hIAPP TG vs NT mice. However, we revealed localised effects of amyloid deposits on islet

capillaries. Specifically, capillaries juxtaposed to amyloid deposits were selectively thicker, showing a 16% increase in diameter, compared with non-amyloid-adjacent vessels, an observation similar to reports of morphological alterations in capillaries close to amyloid deposits in human pancreas [8].

Furthermore, we observed selective abnormalities in NG2-immunoreactive pericytes in amyloid-adjacent capillaries. Pericytes are critical to the maintenance of vascular homeostasis and regulation of blood flow in several tissues including the islet [32]. Pericytes also support beta cell function, as demonstrated by experimental ablation of islet pericytes resulting in impaired insulin release [50]. Our data showed an increase in the number of NG2-positive objects in amyloid-adjacent capillaries. At first glance this increase seems paradoxical but this finding is likely reflective of pericyte dysfunction (i.e. impaired capillary constriction), as suggested by our data showing increased vessel diameter in amyloid-adjacent capillaries. Indeed, islet pericyte proliferation was observed in a recent study using a mouse model of islet fibrosis and this was associated with pericyte dedifferentiation, fibrosis and dysfunction [33]. The increased presence of NG2-positive objects could also be indicative of transdifferentiation from another cell type (e.g. fibroblasts) or of pericyte fragmentation/degeneration. The latter possibility would be in line with reports concerning pancreas from humans with type 2 diabetes, where islet pericyte number is decreased in long-standing disease [32, 46].

The present findings are also in line with a recent transcriptomic study [51] that described significant overlap in differentially regulated genes between islets from hIAPP-overexpressing TG mice and islets from human donors with prediabetes (impaired glucose tolerance and/or impaired fasting glucose) and type 2 diabetes. Of direct relevance to the present study, these findings included differential expression of vasculature-associated genes, such as *Nid1*, *Cxcl12* and *Lgals3bp*, along with a strong differentially regulated gene signature from pericytes. Taken together, these data from several studies suggest a role for hIAPP aggregation in islet pericyte morphology and function, although additional work is needed to elucidate the underlying mechanisms and impact on beta cell function.

In summary, we have demonstrated for the first time that hIAPP aggregation directly impacts islet endothelial cells in vitro and the islet vasculature in vivo, resulting in cytotoxicity, inflammation, capillary enlargement/dilation and disturbances to islet pericytes. These findings suggest that hIAPP-induced vasculopathy could be a previously unrecognised contributor to beta cell failure and cell death in type 2 diabetes and may represent a novel target for therapeutic intervention.

Supplementary Information The online version contains peer-reviewed but unedited supplementary material available at https://doi.org/10.1007/s00125-022-05756-9.

Acknowledgements The authors thank B. Barrow, B. Fountaine, S. Mongovin, M. Peters, C. Schmidt and J. Willard (Seattle Institute for Biomedical and Clinical Research, Seattle, WA, USA) for expert technical support. Portions of the data in this manuscript were presented as abstracts at the 76th and 79th ADA Scientific Sessions in 2016 and 2019, respectively.

Data availability The datasets generated during and/or analysed during the current study are available from the corresponding author on reasonable request.

Funding This work was supported by the Department of Veterans Affairs, VA Puget Sound Health Care System (Seattle, WA), VA Merit Reviews I01-BX004063 (RLH) and I01-BX001060 (SEK) and VA CDA-2 IK2 BX004659 (ATT). The work was also supported by National Institutes of Health grants R01 DK088082 (RLH), GM078114 (DPR), P30 DK017047 (Cellular and Molecular Imaging and Cell Function and Analysis Cores of the University of Washington Diabetes Research Center), P30EY0173 (Electron Microscopy Resource of the University of Washington Core for Vision Research) and the Seattle Institute for Biomedical and Clinical Research. JJC was supported by T32 HL007028. MFH was supported by F32 DK109584 and an ADA Postdoctoral Fellowship. The study sponsors/funders were not involved in the design of the study; the collection, analysis, and interpretation of data; writing the report; and did not impose any restrictions regarding the publication of the report.

Authors' relationships and activities SEK is a member of the editorial board of Diabetologia. All other authors declare that there are no relationships or activities that might bias, or be perceived to bias, their work.

Contribution statement RLH conceived and designed this study, made substantial contributions to the acquisition, analysis and interpretation of data, and revised and gave final approval to the manuscript. JJC, ACA, DJH, RA, NE, ATT, SEK, DPR, SZ and MFH made substantial contributions to the acquisition, analysis and interpretation of data, and revised and gave final approval to the manuscript. RLH is the guarantor and is responsible for the integrity of the work as a whole.

References

1. Olsson R, Carlsson PO (2006) The pancreatic islet endothelial cell: emerging roles in islet function and disease. Int J Biochem Cell Biol 38(5-6):710–714. https://doi.org/10.1016/j.biocel.2006.02.004
2. Richards OC, Raines SM, Attie AD (2010) The role of blood vessels, endothelial cells, and vascular pericytes in insulin secretion and peripheral insulin action. Endocr Rev 31(3):343–363. https://doi.org/10.1210/er.2009-0035
3. Peiris H, Bonder CS, Coates PT, Keating DJ, Jessup CF (2014) The beta-cell/EC axis: how do islet cells talk to each other? Diabetes 63(1):3–11. https://doi.org/10.2337/db13-0617
4. Hogan MF, Hull RL (2017) The islet endothelial cell: a novel contributor to beta cell secretory dysfunction in diabetes. Diabetologia 60(6):952–959. https://doi.org/10.1007/s00125-017-4272-9

5. Lammert E, Gu G, McLaughlin M et al (2003) Role of VEGF-A in vascularization of pancreatic islets. Curr Biol 13(12):1070–1074. https://doi.org/10.1016/s0960-9822(03)00378-6
6. Johansson A, Lau J, Sandberg M, Borg LA, Magnusson PU, Carlsson PO (2009) Endothelial cell signalling supports pancreatic beta cell function in the rat. Diabetologia 52(11):2385–2394. https://doi.org/10.1007/s00125-009-1485-6
7. Hogan MF, Liu AW, Peters MJ et al (2017) Markers of islet endothelial dysfunction occur in male B6.BKS(D)-Lepr^{db}/J mice and may contribute to reduced insulin release. Endocrinology 158(2): 293–303. https://doi.org/10.1210/en.2016-1393
8. Brissova M, Shostak A, Fligner CL et al (2015) Human islets have fewer blood vessels than mouse islets and the density of islet vascular structures is increased in type 2 diabetes. J Histochem Cytochem 63(8):637–645. https://doi.org/10.1369/0022155415573324
9. Shah P, Lueschen N, Ardestani A et al (2016) Angiopoetin-2 Signals Do Not Mediate the Hypervascularization of Islets in Type 2 Diabetes. PLoS One 11(9):e0161834. https://doi.org/10.1371/journal.pone.0161834
10. Lacraz G, Giroix MH, Kassis N et al (2009) Islet endothelial activation and oxidative stress gene expression is reduced by IL-1Ra treatment in the type 2 diabetic GK rat. PLoS One 4(9):e6963. https://doi.org/10.1371/journal.pone.0006963
11. Hogan MF, Hackney DJ, Aplin AC et al (2021) SGLT2-i improves markers of islet endothelial cell function in db/db diabetic mice. J Endocrinol 248(2):95–106. https://doi.org/10.1530/JOE-20-0354
12. Westermark P, Wernstedt C, Wilander E, Hayden DW, O'Brien TD, Johnson KH (1987) Amyloid fibrils in human insulinoma and islets of Langerhans of the diabetic cat are derived from a neuropeptide-like protein also present in normal islet cells. Proc Natl Acad Sci USA 84(11):3881–3885. https://doi.org/10.1073/pnas.84.11.3881
13. Cooper GJS, Willis AC, Clark A, Turner RC, Sim RB, Reid KBM (1987) Purification and characterization of a peptide from amyloid-rich pancreases of type 2 diabetic patients. Proc Natl Acad Sci USA 84(23):8628–8632. https://doi.org/10.1073/pnas.84.23.8628
14. Westermark P, Engström U, Johnson KH, Westermark GT, Betsholtz C (1990) Islet amyloid polypeptide - pinpointing amino acid residues linked to amyloid fibril formation. Proc Natl Acad Sci USA 87(13):5036–5040. https://doi.org/10.1073/pnas.87.13.5036
15. Schneider HM, Storkel S, Will W (1980) Amyloid of islets of Langerhans and its relation to diabetes mellitus (author's transl). Dtsch Med Wochenschr 105(33):1143–1147. https://doi.org/10.1055/s-2008-1070828
16. Clark A, Wells CA, Buley ID et al (1988) Islet amyloid, increased A-cells, reduced B-cells and exocrine fibrosis: quantitative changes in the pancreas in type 2 diabetes. Diabetes Res 9(4):151–159
17. Lorenzo A, Razzaboni B, Weir GC, Yankner BA (1994) Pancreatic islet cell toxicity of amylin associated with type 2 diabetes mellitus. Nature 368(6473):756–760. https://doi.org/10.1038/368756a0
18. Janson J, Ashley RH, Harrison D, McIntyre S, Butler PC (1999) The mechanism of islet amyloid polypeptide toxicity is membrane disruption by intermediate-sized toxic amyloid particles. Diabetes 48(3):491–498. https://doi.org/10.2337/diabetes.48.3.491
19. Jurgens CA, Toukatly MN, Fligner CL et al (2011) Beta-cell loss and beta-cell apoptosis in human type 2 diabetes are related to islet amyloid deposition. Am J Pathol 178(6):2632–2640. https://doi.org/10.1016/j.ajpath.2011.02.036
20. Westwell-Roper C, Dai DL, Soukhatcheva G et al (2011) IL-1 blockade attenuates islet amyloid polypeptide-induced proinflammatory cytokine release and pancreatic islet graft dysfunction. J Immunol 187(5):2755–2765. https://doi.org/10.4049/jimmunol.1002854
21. Masters SL, Dunne A, Subramanian SL et al (2010) Activation of the NLRP3 inflammasome by islet amyloid polypeptide provides a mechanism for enhanced IL-1beta in type 2 diabetes. Nat Immunol 11(10):897–904. https://doi.org/10.1038/ni.1935
22. Meier DT, Morcos M, Samarasekera T, Zraika S, Hull RL, Kahn SE (2014) Islet amyloid formation is an important determinant for inducing islet inflammation in high-fat-fed human IAPP transgenic mice. Diabetologia 57(9):1884–1888. https://doi.org/10.1007/s00125-014-3304-y
23. Westermark P (1972) Quantitative studies on amyloid in the islets of Langerhans. Ups J Med Sci 77(2):91–94. https://doi.org/10.1517/03009734000000014
24. de Koning EJP, Höppener JWM, Verbeek JS et al (1994) Human islet amyloid polypeptide accumulates at similar sites in islets of transgenic mice and humans. Diabetes 43(5):640–644. https://doi.org/10.2337/diab.43.5.640
25. Verchere CB, D'Alessio DA, Palmiter RD et al (1996) Islet amyloid formation associated with hyperglycemia in transgenic mice with pancreatic beta cell expression of human islet amyloid polypeptide. Proc Natl Acad Sci USA 93(8):3492–3496. https://doi.org/10.1073/pnas.93.8.3492
26. Ling W, Huang Y, Huang YM, Shen J, Wang SH, Zhao HL (2020) Pancreatic angiopathy associated with islet amyloid and type 2 diabetes mellitus. Pancreas 49(9):1232–1239. https://doi.org/10.1097/MPA.0000000000001664
27. Hayden MR, Karuparthi PR, Habibi J et al (2008) Ultrastructure of islet microcirculation, pericytes and the islet exocrine interface in the HIP rat model of diabetes. Exp Biol Med (Maywood) 233(9): 1109–1123. https://doi.org/10.3181/0709-RM-251
28. Meier DT, Tu LH, Zraika S et al (2015) Matrix metalloproteinase-9 protects islets from amyloid-induced toxicity. J Biol Chem 290(51): 30475–30485. https://doi.org/10.1074/jbc.M115.676692
29. D'Alessio DA, Verchere CB, Kahn SE et al (1994) Pancreatic expression and secretion of human islet amyloid polypeptide in a transgenic mouse. Diabetes 43(12):1457–1461. https://doi.org/10.2337/diab.43.12.1457
30. Hull RL, Andrikopoulos S, Verchere CB et al (2003) Increased dietary fat promotes islet amyloid formation and beta-cell secretory dysfunction in a transgenic mouse model of islet amyloid. Diabetes 52(2):372–379. https://doi.org/10.2337/diabetes.52.2.372
31. Dai C, Brissova M, Reinert RB et al (2013) Pancreatic islet vasculature adapts to insulin resistance through dilation and not angiogenesis. Diabetes 62(12):4144–4153. https://doi.org/10.2337/db12-1657
32. Almaca J, Weitz J, Rodriguez-Diaz R, Pereira E, Caicedo A (2018) The pericyte of the pancreatic islet regulates capillary diameter and local blood flow. Cell Metab 27(3):630–64 e634. https://doi.org/10.1016/j.cmet.2018.02.016
33. Mateus Goncalves L, Pereira E, Werneck de Castro JP, Bernal-Mizrachi E, Almaca J (2020) Islet pericytes convert into profibrotic myofibroblasts in a mouse model of islet vascular fibrosis. Diabetologia 63(8):1564–1575. https://doi.org/10.1007/s00125-020-05168-7
34. Coate KC, Cha J, Shrestha S et al (2020) SARS-CoV-2 cell entry factors ACE2 and TMPRSS2 are expressed in the microvasculature and ducts of human pancreas but are not enriched in beta cells. Cell Metab 32(6):1028–1040.E4. https://doi.org/10.1016/j.cmet.2020.11.006
35. Aitken JF, Loomes KM, Konarkowska B, Cooper GJ (2003) Suppression by polycyclic compounds of the conversion of human amylin into insoluble amyloid. Biochem J 374(Pt 3):779–784. https://doi.org/10.1042/BJ20030422
36. Young LM, Saunders JC, Mahood RA et al (2015) Screening and classifying small-molecule inhibitors of amyloid formation using ion mobility spectrometry-mass spectrometry. Nat Chem 7(1):73–81. https://doi.org/10.1038/nchem.2129
37. Westwell-Roper C, Denroche HC, Ehses JA, Verchere CB (2016) Differential activation of innate immune pathways by distinct islet

amyloid polypeptide (IAPP) aggregates. J Biol Chem 291(17): 8908–8917. https://doi.org/10.1074/jbc.M115.712455
38. Nackiewicz D, Dan M, He W et al (2014) TLR2/6 and TLR4-activated macrophages contribute to islet inflammation and impair beta cell insulin gene expression via IL-1 and IL-6. Diabetologia 57(8):1645–1654. https://doi.org/10.1007/s00125-014-3249-1
39. Parodi-Rullan R, Ghiso J, Cabrera E, Rostagno A, Fossati S (2020) Alzheimer's amyloid beta heterogeneous species differentially affect brain endothelial cell viability, blood-brain barrier integrity, and angiogenesis. Aging Cell 19(11):e13258. https://doi.org/10.1111/acel.13258
40. Mirzabekov TA, Lin MC, Kagan BL (1996) Pore formation by the cytotoxic islet amyloid peptide amylin. J Biol Chem 271(4):1988–1992. https://doi.org/10.1074/jbc.271.4.1988
41. Porat Y, Kolusheva S, Jelinek R, Gazit E (2003) The human islet amyloid polypeptide forms transient membrane-active prefibrillar assemblies. Biochem 42(37):10971–10977. https://doi.org/10.1021/bi034889i
42. Abedini A, Plesner A, Cao P et al (2016) Time-resolved studies define the nature of toxic IAPP intermediates, providing insight for anti-amyloidosis therapeutics. Elife 5:e12977. https://doi.org/10.7554/eLife.12977
43. Land WG (2015) The role of damage-associated molecular patterns in human diseases: part I - Promoting inflammation and immunity. Sultan Qaboos Univ Med J 15(1):e9–e21
44. Hull RL, Kodama K, Utzschneider KM, Carr DB, Prigeon RL, Kahn SE (2005) Dietary-fat-induced obesity in mice results in beta cell hyperplasia but not increased insulin release: evidence for specificity of impaired beta cell adaptation. Diabetologia 48(7):1350–1358. https://doi.org/10.1007/s00125-005-1772-9
45. Johansson M, Mattsson G, Andersson A, Jansson L, Carlsson PO (2006) Islet endothelial cells and pancreatic beta-cell proliferation: studies in vitro and during pregnancy in adult rats. Endocrinology 147(5):2315–2324. https://doi.org/10.1210/en.2005-0997
46. Takahashi K, Mizukami H, Osonoi S et al (2021) Islet microangiopathy and augmented beta-cell loss in Japanese non-obese type 2 diabetes patients who died of acute myocardial infarction. J Diabetes Investig 12(12):2149–2161. https://doi.org/10.1111/jdi.13601
47. Paris D, Ait-Ghezala G, Mathura VS et al (2005) Anti-angiogenic activity of the mutant Dutch A(beta) peptide on human brain microvascular endothelial cells. Brain Res Mol Brain Res 136(1-2):212–230. https://doi.org/10.1016/j.molbrainres.2005.02.011
48. Wang F, Hull RL, Vidal J, Cnop M, Kahn SE (2001) Islet amyloid develops diffusely throughout the pancreas before becoming severe and replacing endocrine cells. Diabetes 50(11):2514–2520. https://doi.org/10.2337/diabetes.50.11.2514
49. Templin AT, Mellati M, Soininen R et al (2019) Loss of perlecan heparan sulfate glycosaminoglycans lowers body weight and decreases islet amyloid deposition in human islet amyloid polypeptide transgenic mice. Protein Eng Des Sel 32(2):95–102. https://doi.org/10.1093/protein/gzz041
50. Sasson A, Rachi E, Sakhneny L et al (2016) Islet pericytes are required for beta-cell maturity. Diabetes 65(10):3008–3014. https://doi.org/10.2337/db16-0365
51. Blencowe M, Furterer A, Wang Q et al (2021) IAPP-induced beta cell stress recapitulates the islet transcriptome in type 2 diabetes. Diabetologia 65(1):173–187. https://doi.org/10.1007/s00125-021-05569-2